Journal Pre-proof

Annealing effects on photoresist films' mechanical and chemical resistance

Manuel Avellaneda , Andrés Boasso , Martín Sirena , Simón Roa

Please cite this article as: Manuel Avellaneda , Andrés Boasso , Martín Sirena , Simón Roa , Annealing effects on photoresist films' mechanical and chemical resistance, *Surfaces and Interfaces* (2023), doi: https://doi.org/10.1016/j.surfin.2023.103181

Annealing effects on photoresist films' mechanical and chemical resistance

Manuel Avellaneda[1], Andrés Boasso[1], Martín Sirena[2,*], Simón Roa[2,*]

[1]Instituto Balseiro, Centro Atómico Bariloche, Comisión Nacional de Energía Atómica (CNEA), Av. E. Bustillo 9500, S. C. de Bariloche, Argentina.
[2]Instituto de Nanociencia y Nanotecnología (CNEA - CONICET), Nodo Bariloche, Consejo Nacional de Investigaciones Científicas y Técnicas (CONICET) y Centro Atómico Bariloche, Comisión Nacional de Energía Atómica (CNEA), Av. E. Bustillo 9500, R8402AGP San Carlos de Bariloche, Río Negro, Argentina.

(*) Corresponding authors e-mails: martin.sirena@ib.edu.ar (M. Sirena) , **sroadaz8@gmail.com** (S. Roa).

Abstract

Nowadays, photoresist-based films are used by photolithography techniques for the fabrication of micro/nanodevices in the modern nanotechnology industry. The impact of thermal-induced polymerization on the mechanical resistance of these materials is critical for improving both the mechanical and the chemical performance. In this work, we present a systematic study of the annealing effects on the mechanical resistance (thermally-induced material hardening) of MICROPOSIT[TM] photoresist films. The mechanical properties were studied by depth-sensing nanoindentation technique using an atomic force microscope. Results show the films' plastic strain susceptibility decreases as the annealing temperature increases, implying an improvement of their mechanical resistance by thermal-induced polymerization. Strain energy dissipation coefficients decreased from 0.725 up to 0.525 as the annealing temperature was increased from 60 up to 200°C, demonstrating this point. Indentation hardness results were consistent with this behavior, observing an increase from 0.12 up to 0.23 [GPa] for the highest annealing temperature. Annealing-induced hardening seems to be correlated with the films' resistance to wet chemical etching, observing higher chemical resistance for higher annealing temperatures. The observed increase of the mechanical and chemical resistance of the photoresists with annealing becomes of great importance for their application in the development of novel micro and nanostructures.
Keywords: Photoresist Films, Mechanical Properties, Depth-Sensing Nanoindentation, Atomic Force Microscopy.

1. Introduction

Photoresist thin films are used for fabricating different kinds of micro/nanoelectronic devices by photolithography techniques in the nanotechnology industry [1 – 3]. Photoresists are light-sensitive materials (typically polymers dissolved in liquid solutions) commonly spin-coated on substrates to form homogeneous films. Post-annealing treatments below the photoresist boiling temperature are critical for optimum solvent evaporation and efficient polymerization, leading to the growth of compact polymeric structures. This enables to fabricate photoresist films with improved mechanical and chemical properties, which are used as supporting material for the development of novel micro and nanostructures, e.g., electrical nanocontacts [4, 5] and soft lithography molds for biotechnological applications [6, 7].

Despite the relevance of annealed photoresist films as structural materials for photolithography techniques, annealing effects on their mechanical properties have not been studied exhaustively. Few researchers have reported studies related to the photoresist mechanical properties [8 – 13]. On the other hand, the annealing effects on this kind of properties have been marginally studied systematically [8 – 10]. In this context, techniques like Depth-Sensing Nano Indentation (DSNI) have become useful for measuring and analyzing materials' mechanical behavior [14]. Nowadays, Atomic Force Microscopy (AFM)-assisted DSNI has become a powerful tool to study and quantify the mechanical properties of different kinds of micro/nanostructures, especially those considered "soft matter" like polymers and biological materials [15].

Regarding the current relevance of studying thermal-induced mechanical changes in photoresist films, in this work, we present a brief but systematic study of different annealing treatments (from 60 to 200°C) on the mechanical resistance (material

hardening) of MICROPOSIT[TM] photoresist films. AFM-assisted DSNI was used to study and quantify the mechanical properties. Results show the annealing-induced hardening of photoresist films also correlates with their resistance to wet chemical etching resistance to solvents used in microfabrication processes. This fact becomes critical for the use of hardened photoresists for the development of micro and nanostructures. This research provides relevant insights into the characterization of the mechanical and chemical resistance in annealed photoresist films, providing an interesting paradigm to understand the correlation between mechanical and chemical resistance that is critical for the development of efficient photolithography processes.

2. Experimental details

2.1. Fabrication of photoresist films. MICROPOSIT[TM] S1818 positive photoresist solution (from Dow® Shipley - Rohm and Haas Co., boiling point ∼ 146°C) was used to fabricate homogeneous photoresist films on soda-lime glass substrates by spin-coating deposition. Nominally equal (same RPM conditions) spin-coated substrates were annealed at temperatures of 60, 90, 120, 150, and 200°C for 3 minutes on a hot plate at room conditions 90°C is recommended by the manufacturing company. Films with thicknesses (t) about 1.6 – 1.8 [μm] were fabricated. Despite this, experimental evidence indicated that thickness-mediated substrate effects on the films' mechanical behavior are depreciable for the typical indentation depths (h) we are considering ($h < 0.08t$) and these can be neglected, consistent with the 10%-thumb rule for substrate effects in nanoindentation of thin films [16]. Therefore, we consider that the films' mechanical response is thickness-independent, and any observed change in this response is due to annealing effects.

2.2. Mechanical characterization. Photoresist films were mechanically characterized by Depth-Sensing Nano Indentation

(DSNI) technique using the cantilever-bending method [15] with an AFM Dimension[TM] 3100 (from *Veeco Instruments Inc.*) microscope, as shown **Fig. 1**.
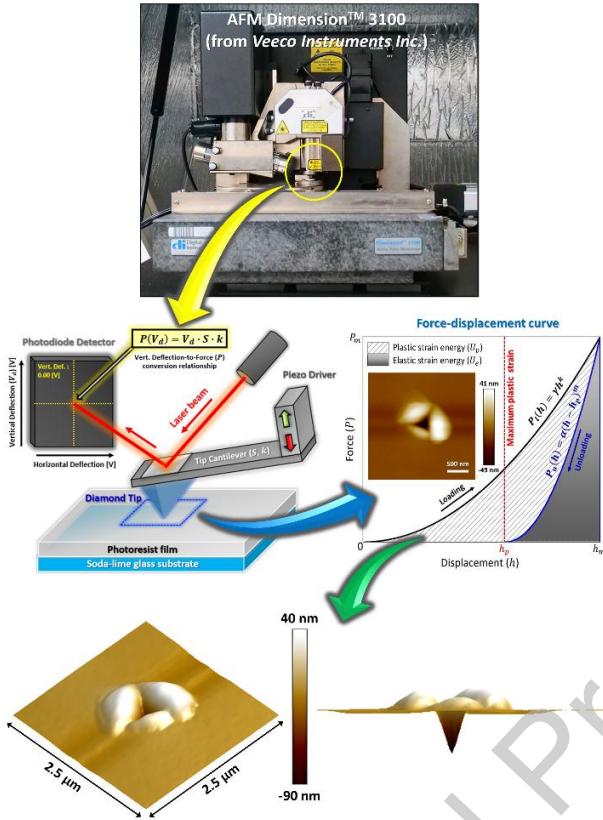

Fig. 1. AFM setup used to perform DSNI measurements, and typical mechanical measurements obtained by this technique

DSNI tests were performed using a commercial AFM- *tapping* silicon probe purchased from *Bruker* Co. (resonance frequency ∼ 322 [kHz]). A cantilever spring constant of 45 ± 6 [N/m] was estimated. The cantilever sensitivity was calibrated on a monocrystalline bulk sapphire sample Sapphire-12M (from *Bruker Co.*), estimating a mean value of 80.4 ± 0.3 [nm/V]. Maximum nominal forces (P) from 3.6 to 14.4 [μN], equivalent to cantilever deflections between 1 and 4 [V], were considered to carry out the mechanical testing. A total of 3x4 indentations matrixes were performed in each sample from 1 (3.6 [μN]) to 4 [V] (14.4 [μN]). The indentation force was increased in a row with a step of 1 [V], and the same sequence was replicated for the next rows.

3. Results and discussion

To achieve a reliable estimation of the films' mechanical properties is important to ensure the indentation dimensions are considerably larger than the surface roughness. This kind of surface defect can impact the accurate estimation of the effective indentation contact area (A_c) and the quantification of the mechanical properties [17], especially when their

dimensions are relatively comparable with the indentation ones [18]. **Fig. 2(a)** shows different AFM images of the annealed photoresist films, observing low average roughnesses (R_a = 0.16 – 0.24 [nm]). Indentation depths achieved in our experiments were ever higher than 20 [nm]. Thus, roughness effects A_c on magnitude were neglected for future data analysis.

Fig. 2(b) shows the indentation tests matrix performed in each sample. The indentation force was increased in a row with a step of 1 [V], and successively replicated for all rows. We generally observed considerable pile-up effects (material strain above the initial surface level) during the indentation tests, which were comparable with the maximum indentation depths. These effects can imply a subestimation of A_c and the overestimation of mechanical properties like hardness (H) and reduced elastic modulus (E_r) [19]. Despite this fact, pile-up effects were not considered in our case.

From **Fig. 2(b)**, we can observe that the plastic indentation response (the indentation footprint) under similar force conditions is reasonably reproducible (considering different rows) for each annealing condition. This fact indicates the homogeneity of the samples' mechanical behavior. In general, an increase in the photoresist film mechanical resistance was observed as the annealing temperature increased. This is evidenced by the 3d-AFM images of the residual plastic indentations shown in **Fig. 2(b)**, where a decrease in the plastic strain is observed for higher annealing temperatures at the same test force condition. This behavior is observed in **Fig. 1(c)**, which shows some examples of the typical $P(h)$ curves measured for the samples and the impact of the annealing conditions on their mechanical behavior.

Fig. 1(c) evidences a clear decrease in the mechanical hysteresis (plastic or residual strain) for higher annealing temperatures. In this case, we can observe a maximum plastic strain of about 70 [nm] for the lowest annealing temperature (60°C) and 30 [nm] for the highest one (200°C), evidencing a clear thermal-induced hardening effect. This is also consistent with the observed decrease of the maximum indentation displacement for higher temperatures. This effect could be associated with a higher polymer densification (more compact polymerization) of the photoresist film at higher temperatures due to the solvent evaporation and consequent polymer chains reorganization by thermal-induced viscous flow, which becomes more important for temperatures nearer to the boiling point [20, 21].

The annealing temperature effects on the films' mechanical resistance can be analyzed using their stress-induced plastic behavior (or "plasticity") as a reference parameter. In the first approach, the films' plasticity can be characterized by their capacity to absorb strain energy, i.e., their capacity to dissipate a fraction of the total mechanical work (energy) involved whole indentation process. This capacity can be calculated by integrating the loading and unloading curves. The integral of the loading and unloading curves correspond to the total (U_t) and recovered/elastic strain energy (U_e), respectively (following the example of previous research [22]). Thus, the strain energy recovery coefficient (U_e/U_t) is defined as:

$$\frac{U_e}{U_t} = \frac{U_e}{U_e + U_p} = \frac{\int_{h_p}^{h_m} P_u(h)dh}{\int_0^{h_m} P_l(h)dh}, \qquad (1)$$

where h_m is the maximum indentation displacement, and h_p is the maximum mechanical hysteresis between the loading $(P_l(h))$ and unloading $(P_u(h))$ curves. Consequently, the strain energy dissipation (or absorption) coefficient is defined as:

$$\frac{U_p}{U_t} = 1 - \frac{U_e}{U_t}, \qquad (2)$$

where U_p is the dissipated strain energy. The U_p/U_t coefficient was calculated for the chosen four load conditions (1, 2, 3 and 4 [V]), observing a dispersion lower than 5 %. Thus, an average value was estimated for each indentation row.
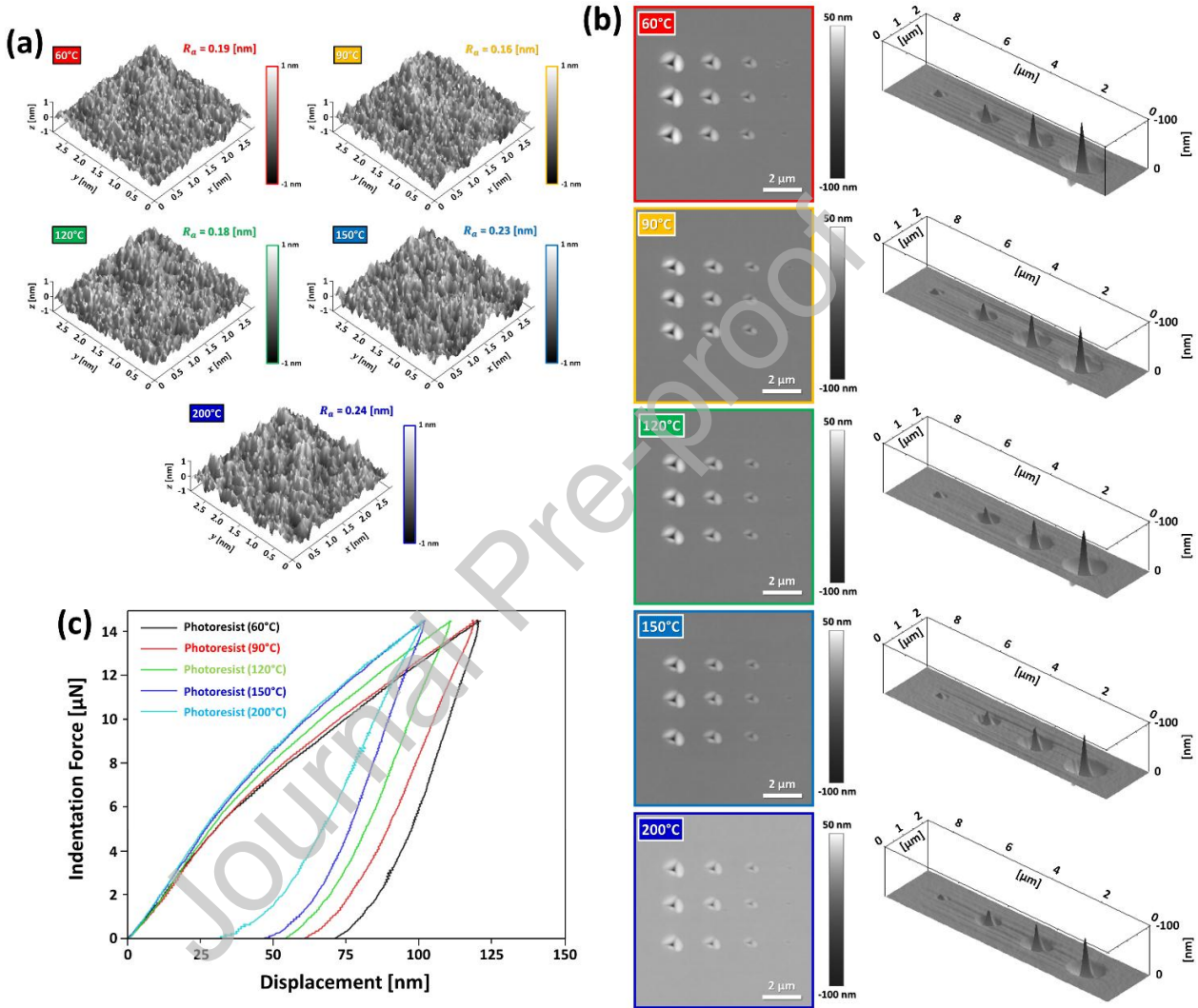

Fig. 2. (a) 3d-AFM images of the photoresist films annealed at different temperatures. A 3 [μm] x 3 [μm] scanning size is shown in each case. **(b)** Indentation tests matrix (3 x 4) performed in each sample from 1 [V] (3.6 [μN]) to 4 [V] (14.4 [μN]). Force was increased in a row with a step of 1 [V], and a similar sequence was done for all rows. 3d projections of the typical indentation sequence observed in a row are also shown. **(c)** Examples of the typically measured indentation curves in photoresist films annealed at different temperatures. In particular, a comparison for a 4 [V]-test is shown.

Fig. 3(a) shows the evolution of the strain energy dissipation coefficient (U_p/U_t) for different annealing temperatures. The U_p/U_t values plotted for each temperature correspond to an average (of 3 values) of the average values measured in an indentation matrix row. These results show that the films' susceptibility to dissipate strain energy tends to decrease as the annealing temperature increases, which is consistent with the decrease of the plastic strain susceptibility (an increase of the mechanical resistance) shown in **Fig. 2(b)** and **2(c)** for higher temperatures. Strain energy dissipation coefficients decreased from 0.725 up to 0.525 as the annealing temperature was increased from 60 up to 200°C. These results show a decrease

of about 28 % of the U_p/U_t ratio for the highest annealing temperature, demonstrating a considerable hardening of photoresist film by thermal effects.
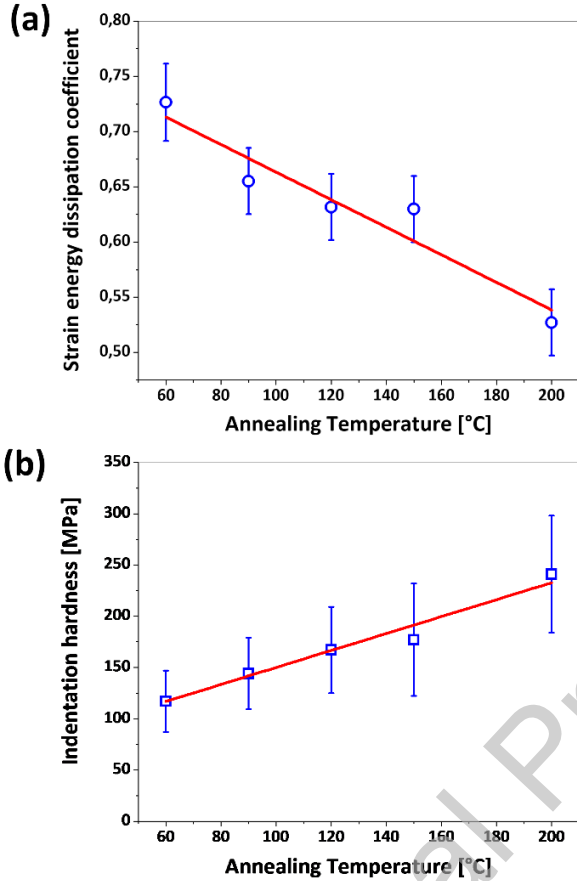
Fig. 3. (a) Evolution of the strain energy dissipation coefficient (U_p/U_t) for different annealing temperatures.**(b)** Evolution of the indentation hardness (H) for different annealing temperatures.

The tendency revealed by analyzing the indentation strain energy was also corroborated by indentation hardness calculations, which were carried out by using the indentation standard formula given by Oliver & Pharr method **[17]**:

$$H = \frac{P_m}{A_c},$$

(3)

where P_m is the maximum force achieved during the indentation test, and A_c is the indentation contact area that can be analytically calculated from the $P(h)$ curves by using accepted standard procedures **[17]**.

Fig. 3(b) shows the evolution of the average H value concerning the increase in the annealing temperature. In agreement with previous observations, an increase in hardness was observed for higher temperatures. Indentation hardness increased from 0.12 up to 0.23 [GPa] for the highest annealing temperature (200°C), representing a considerable improvement of the films' mechanical resistance by annealing effects. These

values are comparable with those observed for other kinds of photoresist materials, which are typically in the order of 10^{-1} [GPa] **[12, 23, 24]**.

Results suggest that low annealing temperatures (60°C or 90°C) involve partial solvent evaporation, implying that the photoresist film holds a fraction of this solvent. Retaining a high volume of liquid solvent (viscous fluid, a quasi-perfect plastic material) can lead to considerable softening effects on the film's effective mechanical response. This fact could explain the lower hardness values observed at this temperature regime. For considerably higher temperatures (200°C), polymer crystallization processes (polymerization) could be taking place and producing stronger chemically-bonded structures by material densification due to the solvent volume reduction. These transitions could be achieved when an energy threshold (thermal energy) is reached **[23]**.

Improving the films' mechanical resistance by annealing mechanisms can modify their resistance to wet chemical etching. This fact was demonstrated by a simple experiment (as shown in **Fig. 4**), which shows the improvement of the chemical resistance achieved for an annealing temperature of 200°C concerning that observed at 90°C. In this case, photoresist films with a photolithography-printed pattern (micrometric lines pattern) were used to assess the photoresist wear resistance.
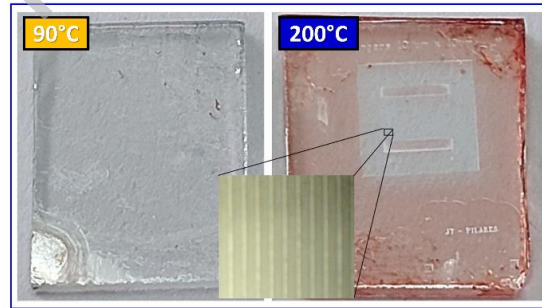
Fig. 4. Different annealed photoresist films with a photolithography-printed pattern after a *wet-etching* process, which consisted of a 3-seconds immersion in a 50 %-acetone/50 %-isopropanol solution.

Fig. 4 shows optical images of the photoresist films annealed at 90 and 200°C after wet etching. Results show a clear correlation between the annealing temperature and the resistance to wet etching, observing that higher temperatures (higher hardness, higher resistance to plastic strain) lead to higher wet etching resistance. This fact suggests that the thermal-induced densification degree of the polymerization, which increases the material mechanical resistance, also increases the material resistance to wet etching processes. In particular, all the photoresist material annealed at 90ºC can be removed from the substrate after wet etching. However, at 200°C, the photolithography pattern remains after the immersion in the chemical etching solution. Results suggest that high-temperature annealing can increase the photoresist resistance to wet etching solutions commonly used for microfabrication processes in photolithography. In this context, annealing treatment engineering enables reasonable

management of photoresist mechanical/chemical optimization, making it an easily-moldable supporting material for fabricating more complex micro and nanostructures.

It should be notice that in polymers, thermal degradation occurs at high temperature. The temperature at which the thermal degradation begins indicates the maximum temperature at which a polymer can be used. Our results indicate that the higher the annealing temperature the higher the mechanical resistance (thought as increased resistance to plastics deformations) and the higher the chemical resistance to solvents used in the microfabrication process. This indicates that as the annealing temperature increases, the performance of the annealed photoresists compared to untreated photoresists, improves. Of course, the upper limit of this effect is given by the thermal degradation of the photoresist.

4. Conclusions

Annealing effects on the mechanical resistance of photoresist films have been successfully studied by the AFM-assisted DSNI technique. Results have shown the films' plastic strain susceptibility decreases as the annealing temperature increases, implying an improvement of their mechanical resistance by thermal-induced polymerization. Strain energy dissipation coefficients decreased as the annealing temperature was increased, demonstrating an annealing-induced hardening effect. Indentation hardness results were consistent with this fact, observing an increase of up to 100 % for the highest annealing temperature concerning the lowest one. Results show a clear correlation between the annealing temperature and the resistance to wet etching, observing that higher temperatures (higher hardness, resistance to plastic strain) lead to higher wet etching resistance. Annealing treatment engineering improves the mechanical and chemical performance of photoresist films to be used in the fabrication of more complex micro and nanostructures by photolithography techniques.

References

[1] C. Luo, C. Xu, Le Lv, Hai Li, X. Huang, Wei Liu, RSC Advances 10 **(2020)** 8385-8395, https://doi.org/10.1039/C9RA08977B

[2] P. Kiefer, V. Hahn, M. Nardi, L. Yang, E. Blasco, C. Barner-Kowollik, M. Wegener, Advanced Optical Materials 8 **(2020)** 2000895, https://doi.org/10.1002/adom.202000895

[3] Z. Zhang, Yu Wang, Qiao Wang, L. Shang, Small 18 **(2022)** 2105116, https://doi.org/10.1002/smll.202105116

[4] Y. Naitoh, T. Sumiya, H. Shima, H. Akinaga, Sensors and Actuators B: Chemical 371 **(2022)** 132531, https://doi.org/10.1016/j.snb.2022.132531

[5] A. Singh, A. Shi, S. A. Claridge, Chemical Communications 58 **(2022)** 13059-13070, https://doi.org/10.1039/D2CC05221K

[6] M. M. Roos, A. Winkler, M. Nilsen, S. B. Menzel, S. Strehle, International Journal of Precision Engineering and Manufacturing-Green Technology 9 **(2022)** 43-57, https://doi.org/10.1007/s40684-021-00367-y

[7] H. Sariogullari, A. Z. Aroguz, Z. Adiguzel, Molecular Biotechnology 65 **(2023)** 786-793, https://doi.org/10.1007/s12033-022-00581-2

[8] R.-C. Chang, F.-Y. Chen, P.-H. Yang, Journal of the Chinese Society of Mechanical Engineers 27 **(2006)** 237-242.

[9] S. Chung, S. Park, Journal of Mechanical Science and Technology 27 **(2013)** 2701-2707, https://doi.org/10.1007/s12206-013-0714-6

[10] A. L. Nikolaev, B. I. Mitrin, E. V. Sadyrin, V. B. Zelentsov, A. R. Aguiar, S. M. Aizikovich, Modeling, Synthesis and Fracture of Advanced Materials for Industrial and Medical Applications, Springer, Cham, **2020**, pp. 137-146, https://doi.org/10.1007/978-3-030-48161-2_9

[11] Y. Wang, Lei Shang, P. Zhang, X. Yan, Ke Zhang, S. Dou, J. Zhao, Yao Li, Polymer Testing 83 **(2020)** 106353, https://doi.org/10.1016/j.polymertesting.2020.106353S

[12] H. Li, J. Chen, Q. Chen, M. Liu, Materials & Design 197 **(2021)** 109239, https://doi.org/10.1016/j.matdes.2020.109239

[13] S. Schweiger, Tim Schulze, S. Schlipf, P. Reinig, H. Schenk, Journal of Optical Microsystems 2 **(2022)** 033501, https://doi.org/10.1117/1.JOM.2.3.033501

[14] Yu. I. Golovin, Physics of the Solid State 63 **(2021)** 1-41, https://doi.org/10.1134/S1063783421010108

[15] A. Magazzù, C. Marcuello, Nanomaterials 13 **(2023)** 963, https://doi.org/10.3390/nano13060963

[16] S. Zak, C. O. W. Trost, P. Kreiml, M. J. Cordill, Journal of Materials Research 37 **(2022)** 1373-1389, https://doi.org/10.1557/s43578-022-00541-1

[17] W. C. Oliver, G. M. Pharr, Journal of Materials Research 7 **(1992)** 1564-1583, https://doi.org/10.1557/JMR.1992.1564

[18] A. C. Campbell, V. Buršíková, J. Martinek, P. Klapetek, International Journal of Mechanical Sciences 161-162 **(2019)** 105015, https://doi.org/10.1016/j.ijmecsci.2019.105015

[19] K. Goto, I. Watanabe, T. Ohmura, Materials & Design 194 **(2020)** 108925, https://doi.org/10.1016/j.matdes.2020.108925

[20] G. M. Bartenev, Journal of Polymer Science Part A-1: Polymer Chemistry 8 **(1970)** 3417-3427, https://doi.org/10.1002/pol.1970.150081204

[21] K. Q. Xiao, L. C. Zhang, International Journal of Mechanical Sciences 44 **(2002)** 2317-2336, https://doi.org/10.1016/S0020-7403(02)00178-9

[22] S. Roa, M. Sirena, C. Redondo, R. Morales, Journal of Physics and Chemistry of Solids 163 **(2022)** 110605, https://doi.org/10.1016/j.jpcs.2022.110605

[23] C. E. Foester, I. T. S. Garcia, F. C. Zawislak, F. C. Serbena, C. M. Lepienski, W. H. Schreiner, Thin Solid Films 411 **(2002)** 256-261, https://doi.org/10.1016/S0040-6090(02)00281-X

[24] M. Zhang, S. Jiang, Y. Gao, J. Nie, F. Sun, Chemical Engineering Journal 390 **(2020)** 124625, https://doi.org/10.1016/j.cej.2020.124625

[25] G. J. Dunderdale, S. J. Davidson, A. J. Ryan, O. O. Mykhaylyk, Nature Communications 11 **(2020)** 3372, https://doi.org/10.1038/s41467-020-17167-8

Graphical Abstract
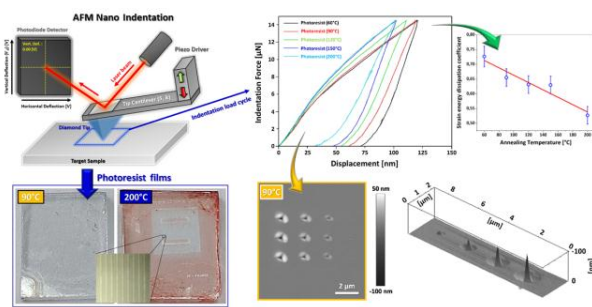
Declaration of interests

☒ The authors declare that they have no known competing financial interests or personal relationships that could have appeared to influence the work reported in this paper.

☐The authors declare the following financial interests/personal relationships which may be considered as potential competing interests: